Appendix 1: Models for co-evolution of Ca and Sr isotopes in seafloor hydrothermal systems

A1.1 Description of the Ca-Sr isotopic exchange model

In modern hydrothermal systems, vent fluids have $^{87}Sr/^{86}Sr$ that is shifted about 80% of the way from the seawater value to the rock value. Assuming that this type of shift is mainly determined by the concentration ratio Sr_{rock}/Sr_{fluid}, the prediction would be that Ca isotopes would be shifted >99% of the way from the seawater value to the rock value, because the analogous ratio Ca_{rock}/Ca_{fluid} is about 15 times larger than for Sr. However, because the system is characterized by fracture flow, there are other effects that come into play in the fracture-matrix interaction that could cause Ca isotopes to be shifted less than expected based on the mass balance and comparison with Sr isotopes (DePaolo, 2006). For ancient seafloor hydrothermal systems, these effects may have been somewhat more pronounced because of differences in the Ca and SO_4 concentrations in seawater (Antonelli et al., 2017). To estimate how much, we use the model of DePaolo (2006), which accounts for the fracture-matrix interaction, although with simplifying assumptions.

Experimental studies and phase stability calculations of altered MORB indicate that calcium and strontium are added to hydrothermal fluids by the dissolution of primary plagioclase and clinopyroxene and removed from hydrothermal fluids by the precipitation of minerals such as anhydrite and amphibole (Pester et al., 2012; Seyfried and Mottl, 1982). These dissolution-precipitation reactions are the principal mechanism for exchanging the isotopes of calcium or strontium between the hydrothermal fluid and rock. Hydrothermal flow through mid-ocean ridges involves both high temperature and low temperature interaction between circulating seawater and basalt (Alt and Teagle, 2003; Coumou et al., 2008; Alt, 1995). Since epidosites form at high temperature, we are mainly interested in the near-axis part of the

hydrothermal system, and with the high temperature evolution of the fluids.

The simple model can be useful in describing isotopic effects in MOR type systems partly because it can be calibrated to observations in modern systems, where the temperature, path length, fluid residence time, and certain isotopic effects can be constrained. The physical parameters in the model (fluid velocity, diffusion coefficient, fracture spacing, and reaction rate describing fluid-rock exchange) can be tuned to generate modern vent fluid $^{87}Sr/^{86}Sr$ with modern seawater as the input fluid. The reason for tuning the model to $^{87}Sr/^{86}Sr$ is because we have those data for the epidosites, and for modern vent fluids, and because Sr isotopes are not fully equilibrated so they provide constraints on the model parameters. The model is then applied to calcium and $\delta^{44}Ca$ by adjusting only the parameters that are different (the concentrations and isotopic compositions of basalt and seawater) but fixing the other parameters.

The model consists of advective transport of fluid in parallel fractures and diffusive transport of pore fluids from the rock matrix to the fractures. Fluid-rock chemical exchange is assumed to occur in the rock matrix and this altered fluid is transported to fractures by diffusion. The model assumes steady-state conditions. The change in the isotopic composition of fluid in an advective-reactive-dispersive system is a function of position and time and depends on fluid velocity in the fracture v (m yr^{-1}), the concentration ratio of the dissolved constituent in the rock (C_s) compared to the fluid (C_l), $K_i = C_s/C_l$, the effective chemical diffusivity of the dissolved element in the inter-fracture porous medium D (m^2yr^{-1}), the bulk reaction rate R (yr^{-1}), and the ratios of density ρ and porosity ϕ between the fluid and rock. The steady-state isotopic ratio versus distance profile of the advecting fluid in the fractures (r_f) can be written in the following form by combining equations 8 and 32 from DePaolo (2006):

$$\frac{dr_{if}}{dx} = \frac{1}{L_{ieq}}(r_{is} - \alpha_i r_{if}) = \frac{RMK_i}{v}\tanh\frac{2L_{id}}{b}(r_{is} - \alpha_i r_{if}) \quad (2)$$

Where L_{ieq} is the isotopic equilibration distance (distance along the fracture flow path) for element i, $M = \frac{\rho_s(1-\phi)}{\rho_f \phi}$ is the rock/fluid mass ratio in the matrix, r_{is} and r_{if} are the isotope ratios in the matrix rock and fracture fluid respectively, v is the advective (fracture) fluid velocity, and b is the fracture spacing. The parameter α_i is the isotopic fractionation factor, which is unity for a radiogenic isotope ratio like $^{87}Sr/^{86}Sr$, but is different from unity for stable isotope systems like oxygen and calcium (Syverson et al., 2018). Equation (2) makes the simplifying assumptions that the fracture fluid concentrations are unchanged along the flow path, the reaction occurs only in the rock matrix, and that the fracture aperture is small compared to the rock volume between fractures (DePaolo, 2006).

The hyperbolic tangent term within the brackets accounts for the diffusive-reactive transport between the matrix and the fracture fluids, which tends to limit the rate of change of the isotope ratio with distance when the (diffusive) equilibration length:

$$L_{id} = \left(\frac{D_i}{RMK_i}\right)^{1/2} \quad (3)$$

is small in comparison to the fracture spacing b. For modern MOR systems, we estimate (Table A1) that the equilibration length for Sr is about 5 to 6 times smaller than the fracture spacing and that for Ca it is about 30 to 40 times smaller. In this case, the ratio of the equilibration lengths for the isotopes of Ca and Sr is approximately equal to $(K_{Ca}/K_{Sr})^{1/2}$. If the matrix diffusion effect were not taken into account, the ratio of the equilibration lengths would reduce to K_{Ca}/K_{Sr}. Hence the fracture-matrix interaction decreases the contrast between Ca and Sr

isotopic evolution in the fracture fluids.

A 1.2 Application to modern MOR systems

The model is applied to modern hydrothermal systems starting with the observation that hydrothermal vent fluids have typical $^{87}Sr/^{86}Sr$ ~0.7037, a value that is shifted about 80-85% of the way from the seawater value (0.70918) to the basalt value (0.7027) (Salters and Stracke, 2004). This observation effectively indicates that L_{eq} for Sr is approximately half the path length of the fluid in the high-temperature hydrothermal system or slightly less (DePaolo, 2006; Turchyn et al., 2013). It is not critical for our argument, but a likely fluid path length through the hydrothermal cell might be 1.4 km (between 1 and 2 km – DePaolo, 2006; Turchyn et al., 2013). If we can now estimate the ratio K_{Ca}/K_{Sr} we can deduce the equilibration length for Ca. There is some uncertainty in estimating this ratio because the fluid Ca and Sr concentrations change as the fluid flows through the system. Using typical seawater and basalt concentrations of the two elements (Table A1) gives $K_{Ca}/K_{Sr}\approx14$. However, because anhydrite precipitation removes Ca in preference to Sr from the fluids before they reach the high-temperature reaction zone, the effective ratio that reaches the high temperature portion of the hydrothermal circulation cell could be higher. This means that the Ca equilibration length is 4 to perhaps 8 times shorter than the Sr equilibration length. This difference is dramatic in terms of extent of isotopic equilibration. If the Sr equilibration distance is, for example, 700 meters, then Sr isotopes will exit the 1400-meter long path having reached 86% of the way toward the rock isotopic values. If the equilibration length for Ca is 4 times shorter, or 175 meters, then Ca isotopes will exit the system having reached 99.97% of the way toward the rock value (or more precisely, toward the steady state value). If instead of the seawater concentrations the typical

vent fluid concentrations are used, then $K_{Ca}/K_{Sr} \approx 5$, and the Ca equilibration distance is only a little less than half that for Sr. This case would suggest that Ca reaches 98% equilibration when Sr is at 86%.

The term "isotopic equilibration" for Ca corresponds to $dr_f/dx = 0$ in equation 2:

$$r_{if} = \frac{r_{is}}{\alpha_i} \tag{4}$$

Written in delta notation, this condition is:

$$\delta^{44}Ca_{fluid} = \delta^{44}Ca_{rock} - \Delta^{44}Ca_{mineral-fluid} \tag{5}$$

In seafloor hydrothermal systems, fluid concentrations of both Ca and Sr are generally increasing as the fluid reacts with the rocks. This means that the flux of Ca from the rock to the fluid is smaller than the flux of Ca from the fluid to the secondary minerals. If the rock-to-fluid flux is higher than the fluid-to-secondary mineral flux by a factor *n*, then the above equation changes to

$$\delta^{44}Ca_{fluid} = \delta^{44}Ca_{rock} - \frac{\Delta^{44}Ca_{mineral-fluid}}{n}$$

For typical seafloor hydrothermal systems the value of *n* is probably about 2 to 4, so any tendency for the fluid to be fractionated relative to the rocks is significantly reduced. The excess flux of Ca and Sr from rock to fluid also causes the equilibration distances to decrease.

Recent work by Sheuermann et al (2019) indicates that the anhydrite-fluid fractionation factor for Ca isotopes is about $\Delta^{44}Ca \approx -0.3$ at 200°C, but approaches zero above 300°C. This experimental result, and the fact that observed fluid $\delta^{44}Ca$ values are close to zero, suggest that overall secondary mineral fractionation at high temperature is negligible.

A 1.4 Ophiolite Hydrothermal Systems

The primary difference between modern hydrothermal systems and those of the mid-Cretaceous and Late Cambrian is that the composition of seawater was different for the older systems (Lowenstein et al., 2014). The seawater concentrations of SO_4 was lower and Ca and Sr were higher. These changes, summarized in Table A1, affect the values of K_{Ca} and K_{Sr}, and hence the equilibration distances (L_{eq}). For Ca, the effect of anhydrite precipitation is muted because the SO_4/Ca ratio was about 0.3 rather than 2.8. The effect of changing seawater chemistry for Sr is more significant because the equilibration length in the modern systems is about ½ the hydrothermal path length so changes in Sr concentration will affect the vent fluid $^{87}Sr/^{86}Sr$. Our estimate is that K_{Sr} for the Cretaceous might have been smaller by about 4 times, which would double the equilibration distance (Table A1). For the Late Cambrian (Betts Cove ophiolite), an even higher seawater (or hydrothermal) Sr concentration is required (e.g. 500 μM; Turchyn et al., 2013). Some estimates of Late Cambrian seawater suggest such high Sr concentrations (Steuber and Veizer, 2002). In the estimated paleo-seawater cases, the ratio of the equilibration lengths of Sr and Ca increase slightly relative to modern. But the value of the equilibration length for Sr increases from smaller than the path length to larger than the path length, causing the high temperature fluids to shift much less toward the rock $^{87}Sr/^{86}Sr$ values. Consequently, the calculated fluid $\delta^{44}Ca$ values are slightly higher than the rock values (Table A2).

The results of the modeling are summarized in Figure A1 (also included in the main text as Figure 3). The model is useful because there are many characteristics that change between modern and ancient systems. The figure shows two sets of fluid evolution curves for

illustration. The solid lines are for $\Delta^{44}Ca_{mineral\text{-}fluid} = 0$, and the lighter dashed lines are for $\Delta^{44}Ca_{mineral\text{-}fluid} = -0.3$ and $n = 2$. The available data suggest that $\Delta^{44}Ca_{mineral\text{-}fluid} = 0$ is the appropriate choice. The result of the modeling is to show that the $\delta^{44}Ca$ of the hydrothermal fluids is likely to be very close to the rock values in all cases. In the most extreme case, the Late Cambrian Betts Cove ophiolite, the fluid $\delta^{44}Ca$ could be about 0.1‰ higher than the rock value. For that example, it is necessary to decrease the reaction rate (R) by 50% to fit the Sr isotope data (Table A2).

A 1.4 High permeability zones and boninites

Cann et al. (2014) have proposed that epidosites in Troodos formed by rapid generation of permeability by mineral dissolution (reaction permeability), and not in fractures. In the Semail ophiolite (MacLeod and Rothery, 1992) and at Betts Cove (Tremblay et al., 1997), pre-obduction normal faults have been documented and fracture flow was the likely pathway for fluid transport during hydrothermal circulation. Since epidosites are massive, and not necessarily formed along fractures, it is certainly possible that they are associated with more permeable local regions in the crust. However, considering the heat and mass transport in modern systems, the bulk of the flow must be through fractures on the kilometer and larger scales (e.g. Hasenclever et al., 2014). If epidosites form in the matrix, it would tend to make the fluids conform even more closely to the Ca isotopic composition of the rocks, since the effective water/rock ratio is likely to be higher.

A 1.5 References

Alt, J.C., Teagle, D.A.H., 2003. Hydrothermal alteration of upper oceanic crust formed at a fast-spreading ridge: mineral, chemical, and isotopic evidence from ODP Site 801. Chemical Geology 201, 191–211. doi:10.1016/S0009-2541(03)00201-8

Alt, J.C., 1995b. Subseafloor Processes in Mid‐Ocean Ridge Hydrothennal Systems, Seafloor Hydrothermal Systems: Physical, Chemical, Biological, and Geological Interactions, Humphris/Seafloor Hydrothermal Systems: Physical, Chemical, Biological, and Geological Interactions. American Geophysical Union (AGU), Washington, D. C. doi:10.1029/GM091p0085

Antonelli, M.A., Pester, N.J., Brown, S.T., DePaolo, D.J., 2017. Effect of paleoseawater composition on hydrothermal exchange in midocean ridges. Proceedings of the National Academy of Sciences 114, 12413–12418. doi:10.1073/pnas.1709145114

Cann, J.R., McCaig, A.M., Yardley, B., 2014. Rapid generation of reaction permeability in the roots of black smoker systems, Troodos ophiolite, Cyprus. Geofluids. doi:10.1111/gfl.12117/pdf

Coumou, D., Driesner, T., Heinrich, C.A., 2008. The Structure and Dynamics of Mid-Ocean Ridge Hydrothermal Systems. Science 321, 1825–1828. doi:10.1126/science.1159582

DePaolo, D.J., 2006. Isotopic effects in fracture-dominated reactive fluid–rock systems. Geochimica et Cosmochimica Acta 70, 1077–1096. doi:10.1016/j.gca.2005.11.022

Hasenclever, J. Theissen-Krah, S., Rüpke, L. H., Morgan, J. P., Iyer, K., Petersen, S. Devey, C. W., 2014, Hybrid shallow on-axis and deep off-axis hydrothermal circulation at fast-spreading ridges. Nature 508, 508-512. doi.org/10.1038/nature13174

Lowenstein, T.K., Timofeeff, M.N., Brennan, S.T., Hardie, L.A., Demicco, R.V., 2001. Oscillations in Phanerozoic Seawater Chemistry: Evidence from Fluid Inclusions. Science 294, 1086–1088. doi:10.1126/science.1064280

MacLeod, C.J., Rothery, D.A., 1992. Ridge axial segmentation in the Oman ophiolite: evidence from along-strike variations in the sheeted dyke complex. Geological Society, London, Special Publications 60, 39–63. doi:10.1144/GSL.SP.1992.060.01.03

Pester, N.J., Reeves, E.P., Rough, M.E., Ding, K., Seewald, J.S., Seyfried, W.E., Jr, 2012. Subseafloor phase equilibria in high-temperature hydrothermal fluids of the Lucky Strike Seamount (Mid-Atlantic Ridge, 37Â°17â€²N). Geochimica et Cosmochimica Acta 90, 303–322. doi:10.1016/j.gca.2012.05.018

Salters, V.J.M., Stracke, A., 2004. Composition of the depleted mantle. Geochem. Geophys. Geosyst. 5, n/a–n/a. doi:10.1029/2003GC000597

Scheuermann, P.P., Syverson, D.D., Higgins, J.A., Pester, N.J., Seyfried, W.E., Jr, 2018.

Calcium isotope systematics at hydrothermal conditions: Mid-ocean ridge vent fluids and experiments in the CaSO4-NaCl-H2O system. Geochimica et Cosmochimica Acta 226, 18–35. doi:10.1016/j.gca.2018.01.028

Seyfried, W.E., Jr, Mottl, M.J., 1982. Hydrothermal alteration of basalt by seawater under seawater-dominated conditions. Geochimica et Cosmochimica Acta 46, 985–1002. doi:10.1016/0016-7037(82)90054-0

Steuber, T., Veizer, J., 2002. Phanerozoic record of plate tectonic control of seawater chemistry and carbonate sedimentation. Geology 30, 1123–1126. doi:10.1130/0091-7613(2002)

Syverson, D.D., Scheuermann, P., Higgins, J.A., Pester, N.J., Seyfried, W.E., Jr, 2018, Experimental partitioning of Ca isotopes and Sr into anhydrite: Consequences for the cycling of Ca and Sr in subseafloor mid-ocean ridge hydrothermal systems. Geochimica et Cosmochimica Acta 236, 160-178.

Tremblay, A., Bédard, J.H., Lauzière, K., 1997. Taconian obduction and Silurian exhumation of the Betts Cove ophiolite, Canadian Appalachians. Journal of Geology 105, 701–716. doi:10.1086/515976

Turchyn, A.V., Alt, J.C., Brown, S.T., DePaolo, D.J., Coggon, R.M., Chi, G., Bédard, J.H., Skulski, T., 2013. Reconstructing the oxygen isotope composition of late Cambrian and Cretaceous hydrothermal vent fluid. Geochimica et Cosmochimica Acta 123, 440–458. doi:10.1016/j.gca.2013.08.015

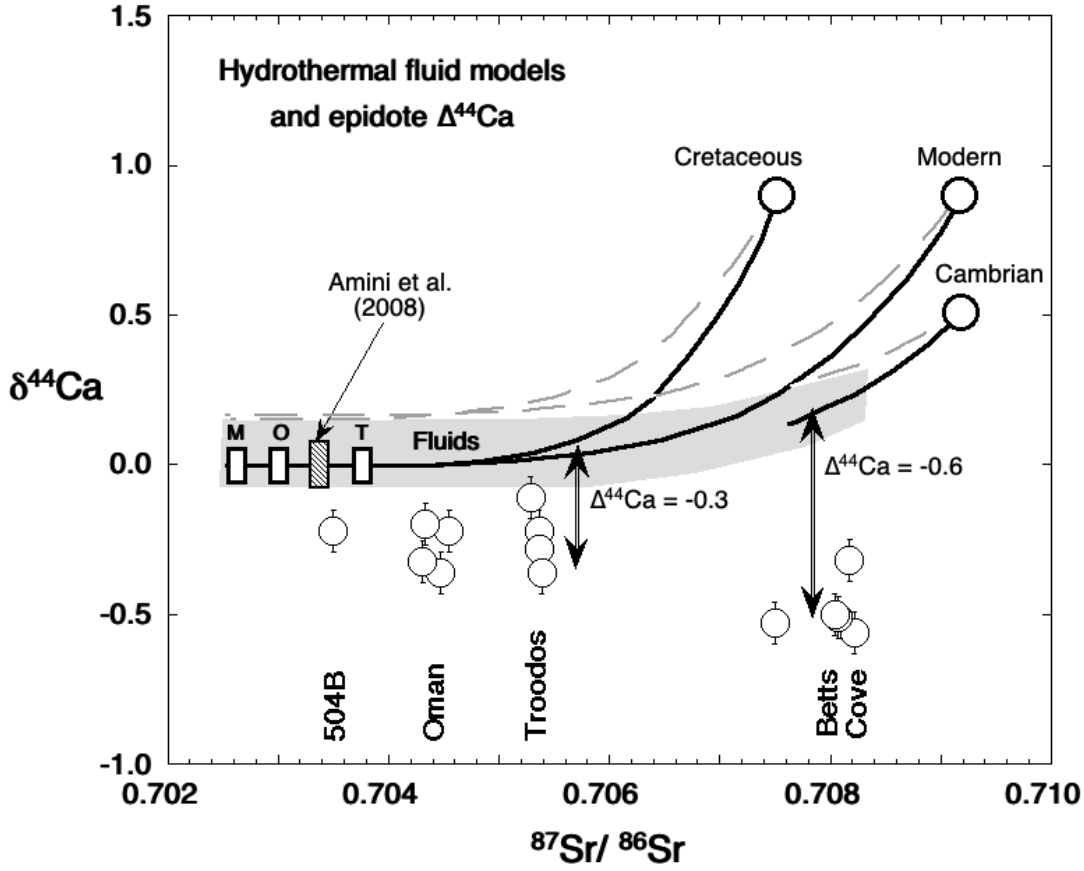

Figure A1: Results of modeling to estimate fluid $\delta^{44}Ca$ from measured epidote $^{87}Sr/^{86}Sr$.

Table A1. Parameters for Sr and Ca exchange model in MOR hydrothermal systems

Parameter	units	Modern	Cretaceous	Late Cambrian
Seawater [Ca]	mM	10.4	30	30
Seawater [Sr]	μM	90	270	450
Seawater [Mg]	mM	54	30	30
Seawater SO_4	mM	28	10	10
Seawater $\delta^{44}Ca$	-	0.9	0.9	0.5
Seawater $^{87}Sr/^{86}Sr$	-	0.70918	0.7075	0.7092
Anhydrite K_{Sr}	-	0.25	0.25	0.25
Anhydrite $\Delta^{44}Ca$ at 200°C		-0.3	-0.3	-0.3
Anhydrite $\Delta^{44}Ca$ at 350°C		0	0	0
Hydrothermal [Ca]	mM	30	50	50
Hydrothermal [Sr]	μM	100	350	600
Fluid Path Length (L_{hyd})	m	1400	1400	1400
Fracture spacing	m	4	4	4
Model Fluid Velocity	m yr^{-1}	35	35	35
Fracture Fluid Velocity	m yr^{-1}	1435	1435	1435
Basalt [Ca]	mM	1750	1750	1750
Basalt [Sr]	μM	1300	1300	1300
Basalt $\delta^{44}Ca$	-	0.0	0.0	0.0
Basalt $^{87}Sr/^{86}Sr$	-	0.7027	0.7037, 0.70295	0.70254
K_{Ca}	-	58.3	35	35
K_{Sr}	-	13	3.7	2.25
D	m^2 yr^{-1}	0.05	0.05	0.05
Matrix Porosity	-	0.01	0.01	0.01
Density ratio	-	2.7	2.7	2.7
M (matrix)		267.3	267.3	267.3
Reaction Rate R	yr^{-1}	0.00005	0.00005	0.000025
L_d (Ca)	m	0.253	0.327	0.462
L_d (Sr)	m	0..536	1.01	1.82
Calculated L_{eq} (Ca)	m	365	473	675
Calculated L_{eq} (Sr)	m	788	1562	3300
Predicted fluid $^{87}Sr/^{86}Sr$		**0.7038**	**0.7050 (Oman) 0.7054 (Troodos)**	**0.7076**
Predicted fluid $\delta^{44}Ca$ at 350°C		**0.00**	**0.05**	**0.12**
Predicted fluid $\delta^{44}Ca$ at 200°C (n=2)		0.15	0.2	0.27
Fraction of rock reacted in 5,000 years		0.25	0.25	0.125